

Synthesis and Characterization of Polyhedral Oligomeric Azido-Octaphenylsilsesquioxane

Haibo Fan, Rongjie Yang

National Laboratory of Flame Retardant Materials, School of Materials, Beijing Institute of Technology, Haidian District, Beijing 100081, People's Republic of China

Received 25 April 2011; accepted 25 July 2011

DOI 10.1002/app.35431

Published online 1 December 2011 in Wiley Online Library (wileyonlinelibrary.com).

ABSTRACT: Polyhedral oligomeric azido-octaphenylsilsesquioxane (N_3 -OPS) was synthesized from octaaminophenylsilsesquioxane (OAPS) via its diazonium salt. The synthesis included nitration of octaphenylsilsesquioxane (OPS) to octanitrophenylsilsesquioxane (ONPS), conversion of ONPS into octaaminophenylsilsesquioxane (OAPS), and conversion of OAPS into N_3 -OPS. The kinetics of the conversion of OAPS into N_3 -OPS were studied by recording the volume of N_2 gas released with the reaction time, which revealed it to be a 1st order reaction. The chemical structures of ONPS, OAPS and N_3 -OPS were characterized by 1H -NMR, GPC, FTIR, ^{29}Si solid NMR, ^{13}C -NMR, XRD, and elemental analysis. It is

proposed that the diazonium salt of OAPS was substituted by the main $-N_3$ group and a few of the $-OH$ groups. The ratio of $-N_3:-OH$ was calculated to be approximately 68:32 in N_3 -OPS on the basis of the elemental analysis and 1H -NMR. XRD suggested that N_3 -OPS was a kind of amorphous compound. The two-step conversion mechanism of OAPS to N_3 -OPS was briefly discussed. TGA results showed that N_3 -OPS was stable at ambient temperature. © 2011 Wiley Periodicals, Inc. *J Appl Polym Sci* 124: 4389–4397, 2012

Key words: azide; octaphenylsilsesquioxane; diazonium salt; kinetics

INTRODUCTION

Polyhedral oligomeric silsesquioxanes (POSS) are well-defined nanosized molecules containing an inorganic silica-like core that is decorated with organic groups. These hybrid nanoparticles have attracted considerable research interest in recent years due to their potential applications in electronics, engineering, material science, and optics.^{1–3} Among various silsesquioxanes, octaphenylsilsesquioxane [OPS, $(PhSiO_{1.5})_8$] has aroused the most interest because it is stable at high temperatures, losing only 5% of its weight on heating to above 436°C,⁴ and gives a high yield of ceramic residue when heated in nitrogen.^{3,5} Many derivatives based on OPS can be prepared by replacement reactions on the phenyl ring. The most important reaction of the phenyl group is nitration, and the nitro group can be quantitatively reduced to $-NH_2$ functions.^{6–9}

The organic azide is a versatile functional group that undergoes a variety of reactions, such as 1,3-

dipolar cycloadditions and rearrangement processes, or acts as a precursor for nitrene chemistry.^{10,11} Recently, the 1,3-dipolar cycloaddition of the reaction between the azido-group and alkynyl-group, known as a “click reaction”, was recognized as a useful synthetic methodology and has been applied in macromolecular chemistry.^{12,13} “Click” chemistry enhances the status of azides greatly, and a number of azido-POSSs have been synthesized and applied in the field of electrochromics,¹³ hydrogels,¹⁴ biomolecules,² liquid crystals,¹⁵ and supramolecules.^{16,17}

The preparation of aryl azide relies on a rather limited selection of transformations.¹¹ They can be prepared from the corresponding amines via their diazonium salts,^{18–20} or from the corresponding amines using triflyl azide.^{10,21,22} However, the preparation of the triflyl azide in the solvent CH_2Cl_2 is a risky undertaking because the nucleophilic substitution on CH_2Cl_2 , leading to azido-chloromethane and/or diazidomethane, can result in explosion. Several laboratories have reported that they have banned the use of halogenated solvents in combination with sodium azide.¹⁰

Octaaminophenylsilsesquioxane (OAPS) was used herein to synthesize azido-octaphenylsilsesquioxane (N_3 -OPS) via its diazonium salts, and a complete characterization of N_3 -OPS is provided. The conversion mechanism and kinetics of the synthesis of N_3 -OPS from OAPS are discussed.

Correspondence to: R. Yang (yrj@bit.edu.cn).

Contract grant sponsor: National High Technology Research and Development Program 863; contract grant number: 2007AA03Z538.

EXPERIMENTAL

Materials and instrumentation

¹H-NMR spectra and ¹³C-NMR spectra were recorded on a Bruker Avance 500 NMR spectrometer operated in the Fourier transform mode. DMSO-d₆ was used as the solvent, and tetramethylsilane (TMS) was used as an internal reference. ²⁹Si solid NMR spectra were recorded on a Bruker Avance 400 NMR spectrometer. Gel permeation chromatography (GPC) measurements were performed on a Waters GPC system, using a Waters 2414 RI detector, Waters HT3, HT4, HT5 columns, a Waters 1515 pump and a Breeze 2 data capture unit. The system was calibrated using polystyrene standards and tetrahydrofuran (THF) was used as the eluent, at a flow rate of 1.0 mL min⁻¹; the detection temperature was 40°C. FTIR spectra were recorded on a Nicolet 6700 IR spectrometer in the attenuated total reflectance mode. The spectra were collected in 32 scans with a spectral resolution of 4 cm⁻¹. The X-ray diffraction (XRD) analysis was achieved using an XPERT-PRP diffractometer system; Cu K α radiation was used with a copper target over the 2 θ range of 0–70°. Thermal gravimetric analysis (TGA) was performed with a NETZSCH 209 F1 thermal analyzer at a heating rate of 10°C/min, and the temperature ranged from 40 to 800°C. Elemental analyses were performed on a Flash EA 1112 automatic elemental analyzer. Octaphenylsilsesquioxane (Si₈O₁₂(C₆H₅)₈, *M* = 1033.2, 97%) was purchased from Hybrid Plastics, Inc. (America). Catalyst Pd/C (5%) was purchased from Baoji Rock Pharmachem Metal (China). Fuming nitric acid (96 wt %), THF, NH₄COOH, NaN₃, NaNO₂, NaHCO₃, and H₂SO₄ (98%) were purchased from Beijing Chemical Works (China).

Octanitrophenylsilsesquioxane

The pathway from OPS to octanitrophenylsilsesquioxane (ONPS) is presented in Scheme 1. ONPS was synthesized using an improvement on Laine's method.²³ HNO₃ (90 mL, 90 wt %) was prepared from fuming nitric acid (82 mL, 96 wt %) and water (8 mL). Octaphenylsilsesquioxane (OPS) (15 g, which is 14.5 mmol) was gradually added to HNO₃ (90 mL, 90 wt %) with stirring at 0°C over 30 min. When the addition was completed, the solution was stirred at 0°C for an additional 30 min and then at room temperature for 20 h. The solution was poured into ice-water (150 g), then a light yellow precipitate was collected by filtration and washed with NaHCO₃ aqueous solution (5 wt %, 300 mL), water (300 mL), and ethanol (150 mL) in turn. The resulting powder was dried in a vacuum at 50°C. The yield was more than 90%. Found: C, 41.30; H, 2.51; N, 8.04%. Calc. for ONPS: C, 41.34; H, 2.30; N,

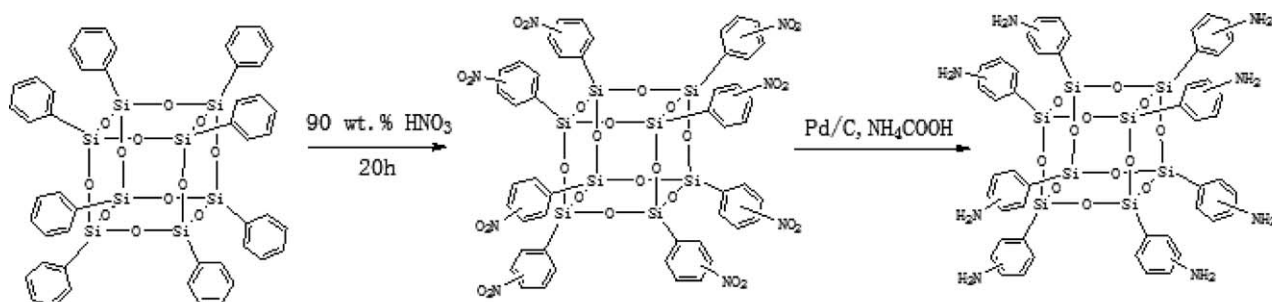
8.04%. FTIR $\nu_{\max}/\text{cm}^{-1}$: 3072 and 1608 (C–H), 1526, and 1348 (NO₂), 1085 (Si–O). δ_{H} (500 MHz; DMSO-d₆): = 8.7–8.5 (1.0H), 8.5–8.0 (5.5H), 8.0–7.7 (2.5H) ppm. ²⁹Si solid NMR: δ = –78.9, –82.3 ppm. δ_{C} (500 MHz; DMSO-d₆): = 152.7, 147.6, 140.3, 137.5, 135.0, 133.8, 130.5, 128.3, 124.7, 122.8 ppm.

Octaaminophenylsilsesquioxane⁶

The pathway from ONPS to OAPS⁶ is presented in Scheme 1. ONPS (5 g, which is 3.59 mmol) and 5% Pd/C (0.61 g, which is 0.287 mmol) were placed in a 250-mL three-necked round-bottomed flask of equipped with a magnetic stirrer and a condenser; then the THF (40 mL) was added. The mixture was heated to 60°C under N₂, then NH₄COOH (7.31g, that is 114.8 mmol) was added quickly to the mixture. The reaction continued for 20 h, and then the solution was filtered through celite and washed with THF (40 mL). The filtrate was combined with ethyl acetate (40 mL), and then washed with an aqueous saturated solution of NaCl (300 mL) and water (100 mL). The organic phase was dried over Na₂SO₄, then poured into hexane (300 mL). The precipitate was collected by filtration. The obtained powder was dried in a vacuum at 50°C. The yield was 68%. Found: C, 48.86; H, 4.11; N, 9.07%. Calc. for OAPS: C, 50.4; H, 4.14; N, 8.91%. FT-IR $\nu_{\max}/\text{cm}^{-1}$: 3456 and 3358 (NH₂), 1596 (C–H), 1073 (Si–O). δ_{H} (500 MHz; DMSO-d₆): = 7.3–6.1 (2.1H, b, H in phenyl group), 5.5–4.4 (1.0H, b, -NH₂) ppm. ²⁹Si solid NMR: δ = –68.3, –77.5 ppm. δ_{C} (500 MHz; DMSO-d₆): = 153.2, 147.9, 135.1, 131.4, 128.6, 121.2, 119.3, 116.4, 114.6, 113.3 ppm.

Azido-octaphenylsilsesquioxane

The pathway from OAPS to N₃-OPS is presented in Scheme 2. (a) Water (28 mL) was placed in a round-bottomed flask equipped with a magnetic stirrer. While stirring concentrated sulfuric acid (98%, 2 mL) was added, followed by OAPS (0.5 g, 0.433 mmol, which is 3.46 mmol of -NH₂). When all the OAPS was dissolved in the H₂SO₄ (aq), the suspension was cooled to 0°C in an ice-salt-water bath. A solution of sodium nitrite (0.25 g, around 1–1.1 eq.) in water (2 mL) was added dropwise over a period of 15 min, and the mixture was stirred for a further 15 min. During this period, the precipitate of the diazonium salt was separated from the initially clear solution. (b) Under vigorous stirring, a solution of sodium azide (1.13 g, 17.3 mmol, 5 eq.) in water (8 mL) was added, and stirring was continued for 60 min. A thick dark brown solid was filtered through celite and washed with water. The powder thus obtained was dried in a vacuum at ambient temperature. The yield was 76%. Found: C, 41.14; H,



Scheme 1 Synthesis of octaaminophenylsilsesquioxane (OAPS).

2.935; N, 16.88%. Calc. for $(\text{N}_3\text{C}_6\text{H}_4\text{SiO}_{1.5})_8$: C, 42.31; H, 2.35; N, 24.84%. FTIR $\nu_{\text{max}}/\text{cm}^{-1}$: 3267 (OH), 2101 (N_3), 1085 (Si—O). δ_{H} (500 MHz; DMSO-d_6): = 10.0–9.0 (1H, b, -OH), 8.0–6.5 (13.5H, b, H in phenyl group) ppm. ^{29}Si solid NMR: δ = -69.8, -79.3 ppm. δ_{C} (500 MHz; DMSO-d_6): = 162.5, 138.7, 135.9, 130.4, 129.6, 124.1, 121.2, 118.4 ppm.

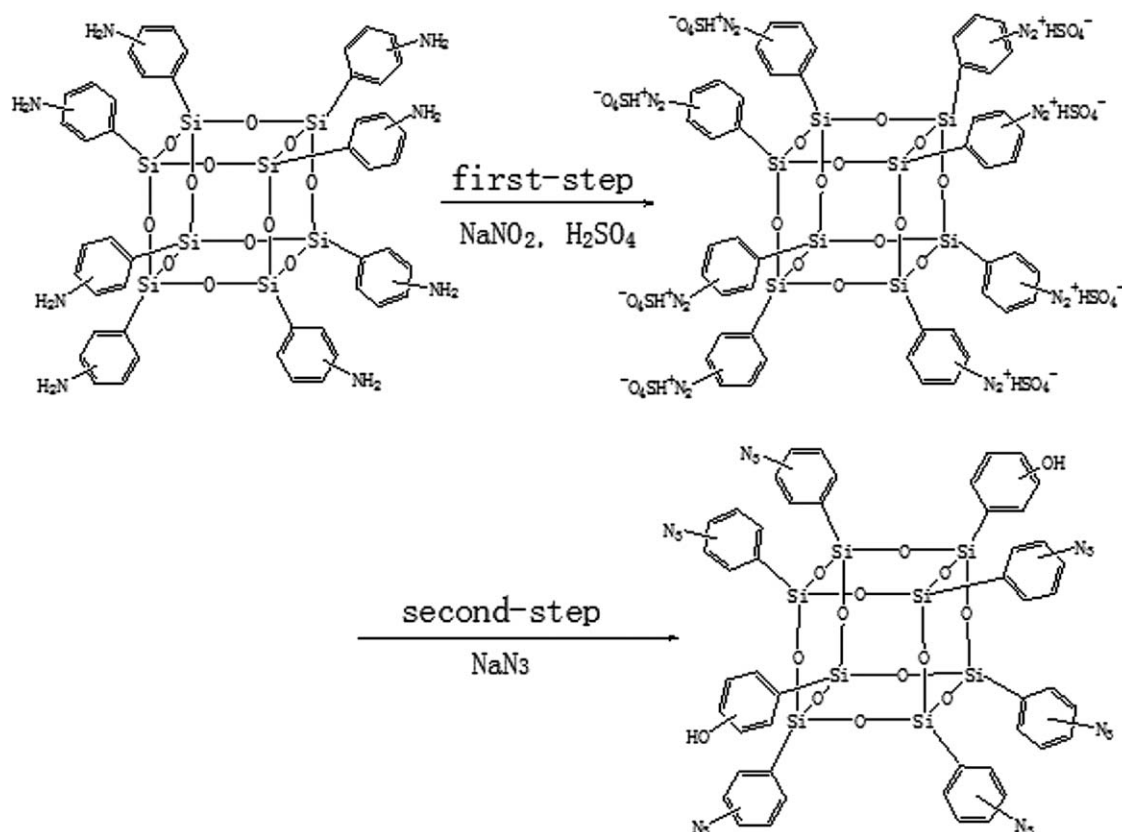
RESULTS AND DISCUSSION

Reaction conditions

The procedure reported by Laine et al.⁶ for the synthesis of ONPS was improved. The result of this improved procedure was that every phenyl unit on

ONPS had only one nitro group.²³ Then ONPS was quantitatively transformed to OAPS by a hydrogen-transfer reduction in the presence of NH_4COOH and Pd/C catalyst (Scheme 1).²⁴ To synthesize the N_3 -OPS cube a simple synthetic strategy was used (Scheme 2). An aqueous solution of sodium nitrite NaNO_2 in concentrated sulfuric acid was used as a very effective diazotizing medium at 0°C. The resulting diazonium salt ($-\text{N}_2^+\text{HSO}_4^-$) was replaced mainly by the $-\text{N}_3$ group attached to the aromatic ring by the release of N_2 .

In this reaction, the volume of H_2SO_4 , the first-step diazo time using $\text{NaNO}_2 + \text{H}_2\text{SO}_4$, the quantity of NaN_3 and the second-step azide substitution time play important roles in increasing the conversion of



Scheme 2 Two-step synthesis of azido-octaphenylsilsesquioxane (N_3 -OPS).

TABLE I
Reaction Conditions and Fractions of Nitrogen in N₃-OPS (at 0°C)

H ₂ SO ₄ (mL)	First-step diazo time (min)	NaN ₃ (g)	Second-step azide substitution time (h)	N (wt. %)
2	45	0.752 (3 eq.)	1	14.63
2	45	0.752 (3 eq.)	3	15.10
4	45	0.752 (3 eq.)	1	15.14
2	45	1.253 (5 eq.)	1	15.10
2	15	1.253 (5 eq.)	1	16.88

the diazonium ion $-\text{N}_2^+\text{HSO}_4^-$ into $-\text{N}_3$. A large fraction of nitrogen in N₃-OPS means a high conversion of the azide group. The reaction conditions are shown in Table I. Increasing the volume of H₂SO₄ would lower the concentration of OH⁻; decreasing the first-step diazo time would reduce the time of conversion of the diazonium ions into $-\text{OH}$. But if the diazo time is too short, the diazo reaction would not be complete. It was verified that reducing the first-step diazo time could effectively increase the fraction of the $-\text{N}_3$ group. The theoretical fraction of N element in octaazidophenylsilsesquioxane is 24.84%. According to the elemental analysis, the degree of $-\text{N}_3$ substitution of $\sim 68\%$ under the reaction conditions in the last row in Table I was obtained by dividing the experimental value 16.88% by the theoretical value 24.84%.

Kinetic analysis

Figure 1 is a schematic diagram of the simple reaction equipment used in the conversion of OAPS into

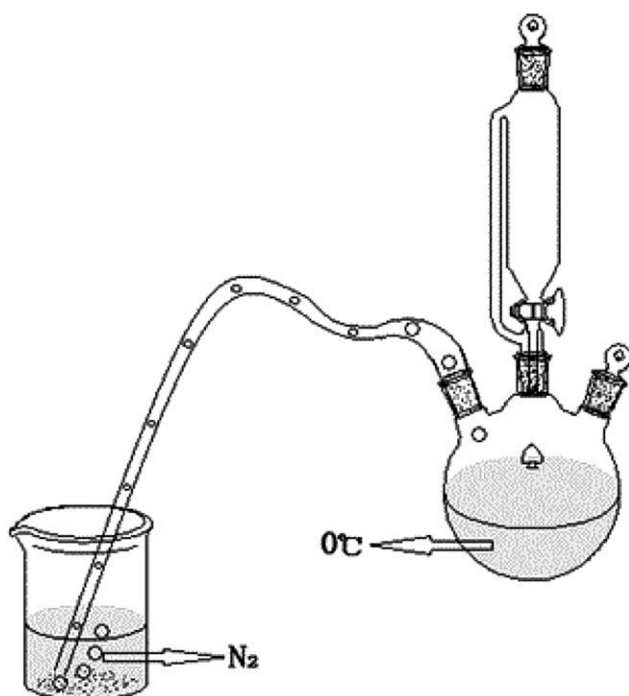


Figure 1 Schematic diagram of reaction equipment.

N₃-OPS. The kinetic analysis was based on the release rate of the nitrogen gas during the conversion of diazonium ions into $-\text{N}_3$ or $-\text{OH}$.²⁵ The temperature was controlled at 0°C. The nitrogen gas was released in bubbles as the reaction progressed, so the number of bubbles (n) could be counted. The numbers of bubbles recorded after adding NaNO₂ and NaN₃ are shown in Figures 2 and 3, respectively, reflecting the kinetics of the reactions. The nitrogen release after adding NaNO₂ proves that the diazonium ions were converted into $-\text{OH}$. After adding NaN₃, the reaction rate gradually changed from fast to slow. After 1 h (3600 s), the reaction rate became very slow.

Suppose that $C(\text{N}_2^+)$ represents the concentration of diazonium ions ($-\text{N}_2^+\text{HSO}_4^-$). When the first bubble emerged after the addition of NaN₃, $C(\text{N}_2^+)_0$ could be considered as 100%, while at the end of the reaction $C(\text{N}_2^+)$ it would be 0%. During the reaction process, $C(\text{N}_2^+)$ at time t could be calculated using the number (n) of bubbles and the total number (n_0) of bubbles: $C(\text{N}_2^+) = 1 - n/n_0$. It should be pointed out that in the reaction system NaN₃ is present in a significant excess (5 eq.), and therefore the concentration of NaN₃ was considered not to influence the reaction rate. Figure 4 shows a logarithmic relationship between $C(\text{N}_2^+)$ and t under the reaction

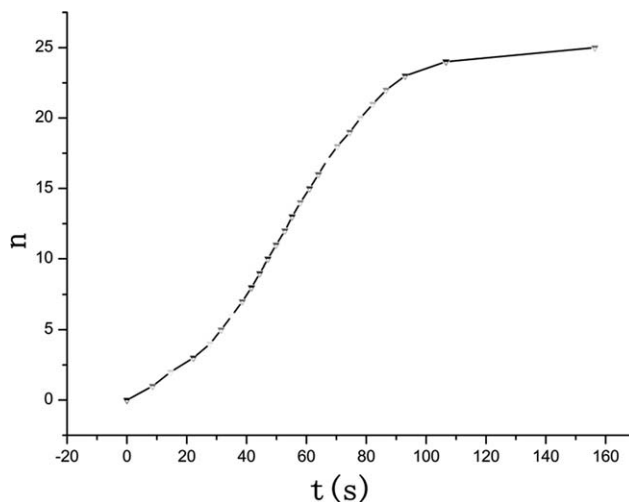


Figure 2 Relationship between the number of bubbles of nitrogen (n) and reaction time (t) after adding NaNO₂.

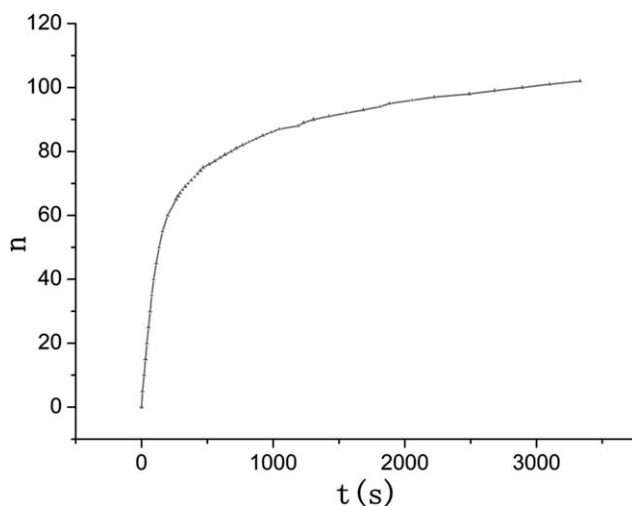


Figure 3 Relationship between the number of bubbles of nitrogen (n) and reaction time (t) after adding NaN_3 .

conditions in the last row in Table I. It is interesting that the relationship from 3 to 30 min was linear; the fitting equation was $\ln[c(\text{N}_2^+)/c(\text{N}_2^+)_0] = -0.7579 - 1.44 \times 10^{-3}t$ with a correlation coefficient of 0.9985.

Structure of polyhedral oligomeric silsesquioxanes

The structures of ONPS, OAPS and N_3 -OPS were confirmed by $^1\text{H-NMR}$ spectra (DMSO-d_6) (Fig. 5). The aromatic protons of benzene emerged at 7.27 ppm. Because of the electron withdrawing effect of $-\text{NO}_2$, the aromatic protons of ONPS emerged at 8.7–7.7 ppm. No peak emerged over 9.0 ppm, which means there was no benzene that had two $-\text{NO}_2$ in ONPS. At the same time, the experimental value of N element in ONPS was 8.04%, which means every benzene possessed only one $-\text{NO}_2$ in ONPS. The reduction process led to two changes in the OAPS spectrum. While the N–H protons appeared at 5.5–4.5 ppm as new peaks, the aromatic protons

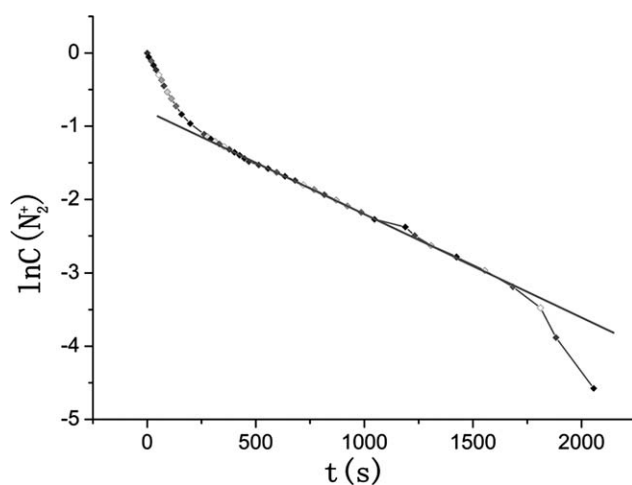


Figure 4 Relationship between $\ln C(\text{N}_2^+)$ and time (t).

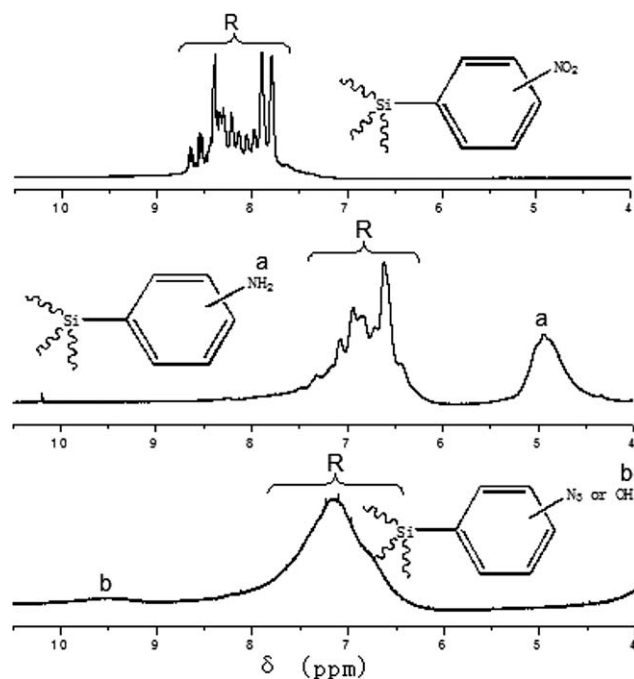


Figure 5 $^1\text{H-NMR}$ spectra of ONPS, OAPS and N_3 -OPS (R: aromatic protons).

appeared at high magnetic fields in the 7.3–6.1 ppm range. The ratio of N–H protons to aromatic C–H protons was 1:2.1, indicating the quantitative reduction of the nitro groups to amino groups. The efficient transformation of OAPS to N_3 -OPS was also evident from the $^1\text{H-NMR}$ spectra because the peak for the N–H protons disappeared completely, which meant that all of the amino groups were converted. At the same time, a small peak at 9–10 ppm was observed. Because the diazonium salt was sensitive to the ions in the system, the OH^- ions in the acidic solution could substitute the diazonium ions as well. Thus the peak at 9–10 ppm in the $^1\text{H-NMR}$ spectrum of N_3 -OPS was attributed to the protons in the $-\text{OH}$ of phenol caused by the conversion of diazonium ions into $-\text{OH}$. According to the peak areas of 6.5–8 ppm and 9–10 ppm (1.00 and 13.51), the degree of $-\text{OH}$ substitution was $\sim 29.6\%$ ($(32/13.51)/8 = 29.6\%$). So the degree of $-\text{N}_3$ substitution was 70.4%. This result is similar to the calculation from the elemental analysis.

Figure 6 shows the GPC of ONPS, OAPS, and N_3 -OPS. The theoretical molecular weight of ONPS is very close to the measured value, which indicates there is only one nitryl group, rather than two nitryl groups for every phenyl group in the ONPS molecule. The molecular weight of OAPS was incorrect because the theoretical molecular weight of OAPS (1153) is smaller than the lowest measurement limit (1200). The GPC revealed that the polydispersity indexes (PDI) of ONPS and OAPS were 1.01 and 1.02, respectively, confirming the purity of the ONPS

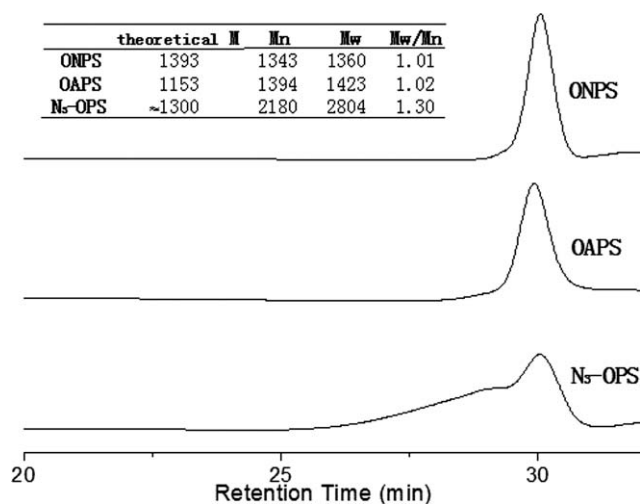


Figure 6 GPC results for ONPS, OAPS, N_3 -OPS in THF at 40°C.

and OAPS and their stable cage structures. But for the N_3 -OPS, there was a wide shoulder peak in the evolution curve, and the PDI was 1.30. This probably caused by the hydrogen bonding of the N_3 -OPS, because nearly 30% of the $-NH_2$ were changed to $-OH$. The molecular weight was around 3000 if the retention time was 27.5 in the GPC. So two, three or even more N_3 -OPS molecules were associated via hydrogen bonding.

The FTIR spectrum of ONPS exhibited strong symmetric and asymmetric $\nu(N=O)$ peaks at 1348 and 1526 cm^{-1} , as shown in Figure 7. These peaks disappeared completely after reduction, and the new broad symmetric and asymmetric $\nu(N-H)$ peaks appeared at 3358 and 3450 cm^{-1} . After the transformation of OAPS to N_3 -OPS, a strong $-N_3$ vibration at 2101 cm^{-1} appeared in the spectrum of N_3 -OPS, which indicated that the $-N_3$ substituted for $-NH_2$. At the same time, a wide $-OH$ vibration at

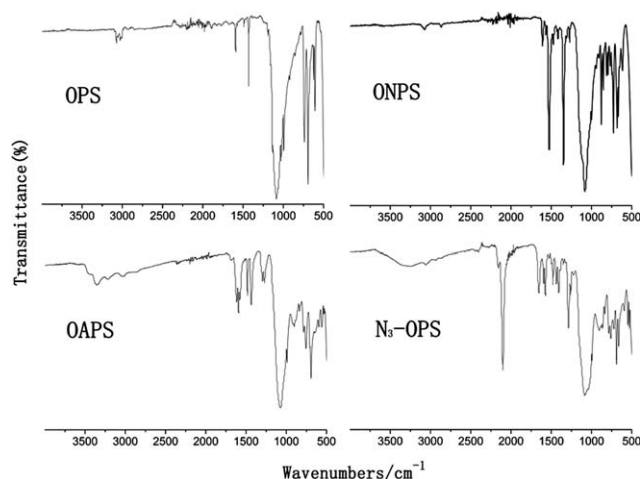


Figure 7 FTIR spectra of OPS, ONPS, OAPS, and N_3 -OPS.

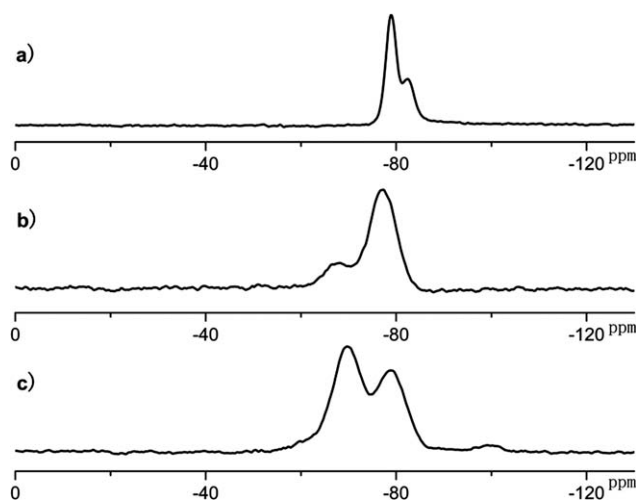


Figure 8 ^{29}Si solid NMR spectra of (a) ONPS, (b) OAPS, and (c) N_3 -OPS.

3267 cm^{-1} existed, which was caused by the appearance of phenol. It was noticeable that all these functionalized OPS disclosed characteristics of $\nu(Si-O-Si)$ stretching signals between 1085–1073 cm^{-1} with relatively high intensity. These supported the 1H -NMR data.

Figure 8 shows the ^{29}Si solid NMR spectra of ONPS, OAPS, and N_3 -OPS. Two peaks were observed at -79.8 and -82.3 ppm of ONPS corresponding to the isomers of para- and meta- NO_2 on the phenyl ring, respectively. The two peaks in the ^{29}Si solid NMR spectrum of OAPS are also evidence of the two isomers. After the azide substitution process, the two isomers' peaks at -69.8 and -79.3 ppm also emerged in the spectrum of N_3 -OPS. However, the area ratios of the two peaks were significantly different for ONPS and OAPS. This is attributable to the Si being connected to the phenyl- N_3 groups or the phenyl-OH groups, respectively.

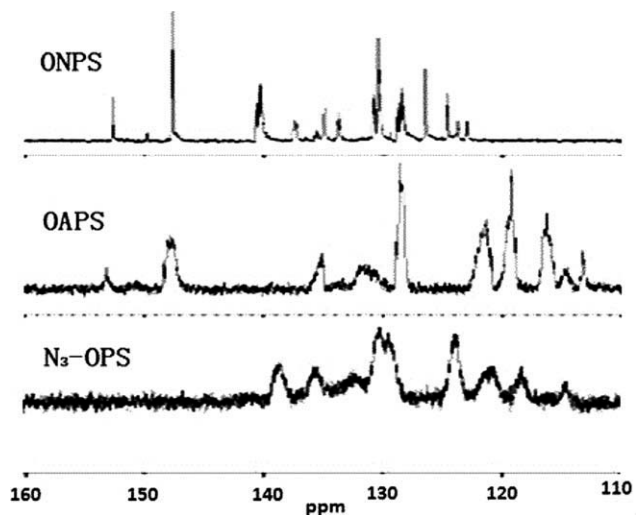


Figure 9 ^{13}C -NMR spectra of ONPS, OAPS, and N_3 -OPS.

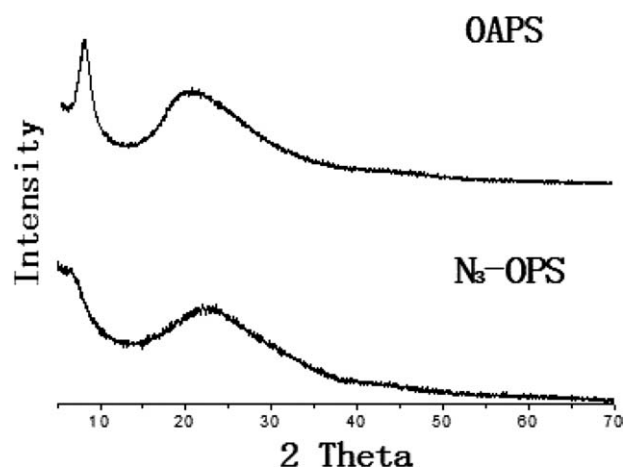


Figure 10 Wide-angle XRD patterns of OAPS and N_3 -OPS.

Figure 9 shows the ^{13}C -NMR spectra of ONPS, OAPS and N_3 -OPS. The ^{13}C -NMR spectra of ONPS and OAPS here are similar to those reported in Refs. 9 and 26 where no detailed analyses of the ^{13}C -NMR spectra of ONPS and OAPS were given. In the ^{13}C -NMR spectra of N_3 -OPS, shift of the resonance peaks and the disappearance of the peaks at around 150 ppm compared with the spectra of OAPS should be attributed to $-\text{N}_3$ and possible $-\text{OH}$ groups on the phenyl group. Some resonance peaks should merge together. The connection between these resonance peaks and the particular C positions in these molecules has not been analyzed in detail. Moreover, the ^{13}C -NMR is not suitable for a quantitative analysis of carbon in different chemical environments.

The structure of N_3 -OPS was also characterized by XRD (Figs. 10 and 11). The wide-angle XRD pattern of OAPS was similar to those in Refs. 9 and 27. The wide-angle XRD pattern of N_3 -OPS in Figure 10 shows a wide amorphous diffraction peak. The diffraction

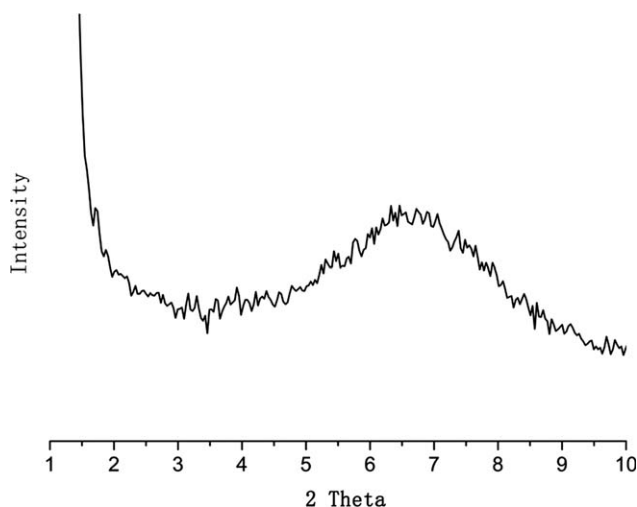
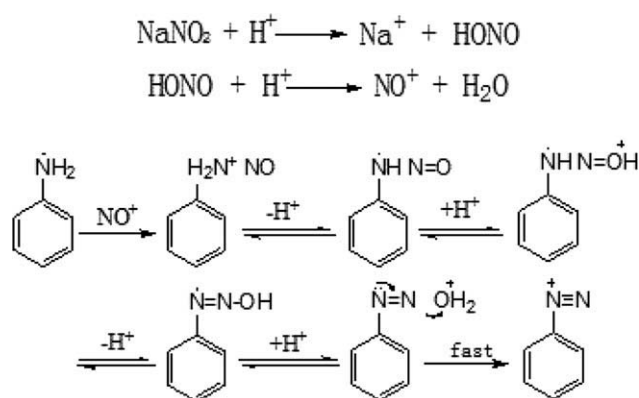


Figure 11 Small-angle XRD pattern of N_3 -OPS.

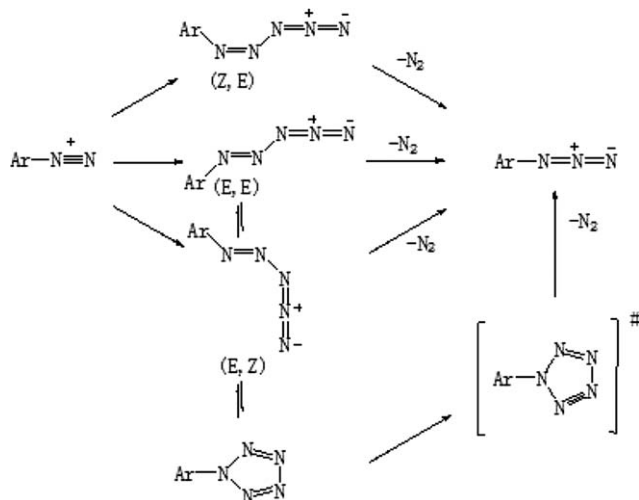


Scheme 3 Mechanism of diazo reaction.

peak of OAPS at $2\theta = 7.75^\circ$ means a d -spacing of $\approx 11 \text{ \AA}$ (by Bragg's equation). The small-angle XRD pattern of N_3 -OPS in Figure 11 shows a peak at $2\theta = 6.5^\circ$ corresponding to a d -spacing of 14 \AA . The diffraction peak is related to the local order of the POSS cage structure. The greater d -spacing of N_3 -OPS indicates a bigger cage than that in OAPS.

Conversion mechanism of octaaminophenylsilsesquioxane into azido-octaphenylsilsesquioxane

The conversion of OAPS to N_3 -OPS undergoes two-steps: formation of the diazonium salt ($-\text{N}_2^+\text{HSO}_4^-$) and substitution of the $-\text{N}_3$ group. The mechanism of the diazo reaction (formation of the diazonium salt) is shown in Scheme 3. First, the weak electrophilic nitrosyl positive ion was produced through dehydration of the protonated nitrous acid. Second, N -nitrosamines were created through interaction between the nitrosyl positive ion and the amino group of the primary aromatic amine. Third, diazo acids were produced by keto-enol tautomerism of



Scheme 4 Conversion mechanism of diazonium ion to azide.

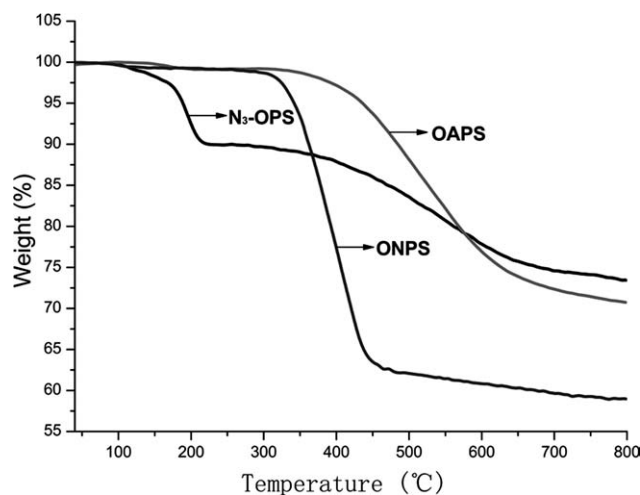


Figure 12 TGA curves of ONPS, OAPS, and N_3 -OPS (N_2 atmosphere).

N-nitrosamines. Finally, diazonium salts were formed by the protonation and dehydration of the diazo acids.

The reaction of aryl diazonium salt to aryl azide is the oldest method for the preparation of azides.¹¹ Aryl diazonium salt reacts directly with azide ions without catalysts to form the corresponding aryl azide. This reaction occurred with the attack of the azide ion on the diazonium ion, with formation of aryl pentazoles and its subsequent products (Scheme 4).¹¹ It is sufficiently rapid even at low temperatures. There is a general consensus that the mechanism involves an intermediate pentazene and that the pentazole loses dinitrogen.^{11,28} In the conversion process of the diazonium ion, the azide ion is not unique. The OH⁻ in the acidic solution could substitute the diazonium ions.²⁹ Therefore in this reaction system, the diazonium ion could be substituted by OH⁻ to form a phenol group.

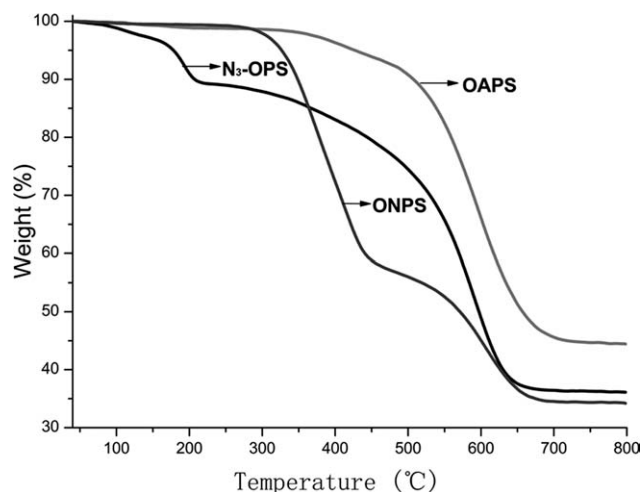


Figure 13 TGA curves of ONPS, OAPS, and N_3 -OPS (air atmosphere).

TABLE II
Results of TGA of ONPS, OAPS, and N_3 -OPS

Sample	In N_2		In air	
	T_{d5} ($^{\circ}C$)	Residue (%)	T_{d5} ($^{\circ}C$)	Residue (%)
ONPS	342	59.01	327	34.21
OAPS	440	71.12	427	44.42
N_3 -OPS	189	73.20	178	36.12

Thermal stability of azido-octaphenylsilsequioxane

TGA curves of ONPS, OAPS and N_3 -OPS in N_2 atmosphere are presented in Figure 12. We observed that the T_{onset} (189 $^{\circ}C$) of N_3 -OPS at 5% weight loss was much lower than that of ONPS and OAPS. It could be seen that the weight loss in the temperature range of 130–220 $^{\circ}C$ was fast, probably caused by N_3 -OPS losing $-N_3$ groups. A slow weight loss between 220–800 $^{\circ}C$ followed, which corresponded to the loss of phenyl groups. The N_3 group was easily removed from the phenyl group with increasing temperature. Removal of the N_3 group produced free radicals, which is advantageous to cause the cross-linking reactions in the condensed phase to form more residues. So, the residue of N_3 -OPS at 800 $^{\circ}C$ was 73.4%, which was higher than that of ONPS and OAPS.

The TGA curves of ONPS, OAPS, and N_3 -OPS in air atmosphere are presented in Figure 13 and the TGA results of ONPS, OAPS, and N_3 -OPS are shown in Table II. The T_{onset} of the same POSS was similar in N_2 and air atmosphere, but the residue in N_2 atmosphere was much higher than the residue in air atmosphere due to the presence of O_2 . There are two mass loss steps in the TGA curve of N_3 -OPS in the air atmosphere, standing for the loss of the organic substitution groups and the breakage of the POSS structure. The temperature of maximum mass loss rate of the second mass loss step was 588 $^{\circ}C$, which was accorded to the Refs. 30 and 31. And in the air atmosphere, the residue yields at 800 $^{\circ}C$ for ONPS, OAPS, and N_3 -OPS were 34.21, 44.42, and 36.12%, while the theoretical residue yields for ONPS, OAPS, and N_3 -OPS were 36.75, 44.41, and 39.48%. So the ceramic yields estimated by the TGA results were consistent with the theoretical results.

CONCLUSIONS

This article describes a facile and inexpensive way to prepare N_3 -OPS via its diazonium salt. ONPS and OAPS were prepared first. Reducing the time of the first-step diazo reaction by $NaNO_2$ and H_2SO_4 effectively increased the $-N_3$ substitution degree. The kinetics of conversion of OAPS into N_3 -OPS were studied by recording the volume of N_2 gas released

with reaction time, revealing the reaction to be 1st order. The chemical structures of ONPS, OAPS, and N₃-OPS were characterized by ¹H-NMR, GPC, FTIR, ²⁹Si solid NMR, ¹³C-NMR, XRD, and elemental analysis. ¹H-NMR and FTIR revealed that the diazonium salt ($-N_2^+HSO_4^-$) of OAPS was substituted by the main $-N_3$ groups and a few of the $-OH$ groups. And the ratio of $-N_3$: $-OH$ was calculated to be ~ 68 : 32 in the N₃-OPS compound. XRD suggested that N₃-OPS is a kind of amorphous compound, and has the greater d-spacing than OAPS, demonstrating the larger POSS cage. The two-step conversion mechanism of OAPS to N₃-OPS was briefly discussed. TGA results showed that N₃-OPS is stable at ambient temperature in either N₂ or air atmosphere. In future, an attempt should be made to prepare pure octaazidophenylsilsesquioxane by removing hydroxyl.

References

1. Paul, D. L.; Franck, R. *Adv Organomet Chem* 2008, 57, 30.
2. Sebastian, F.; Dirk, H.; Viktor, B. *Org Biomol Chem* 2010, 8, 2212.
3. David, B. C.; Paul, D. L.; Franck, R. *Chem Rev* 2010, 110, 2081.
4. Du, J. K.; Yang, R. J. *Fine Chemicals* 2006, 22, 409.
5. Fina, A.; Tabuani, D.; Carniato, F. *Thermochim Acta* 2006, 440, 36.
6. Ryo, T.; Yasuyuki, T.; Michael, Z. *J Am Chem Soc* 2001, 123, 12416.
7. Zhang, J.; Xu, R. W.; Yu, D. S. *J Appl Polym Sci* 2007, 103, 1004.
8. Kim, S. G.; Choi, J.; Tamaki, R. *Polymer* 2005, 46, 4514.
9. Shanmugam, N.; Muthukaruppan, A.; Ian, H. *Acta Mater* 2010, 58, 3345.
10. Alexander, T.; Zorana, R.; Oliver, S. *Tetrahedron Lett* 2006, 47, 2383.
11. Stefan, B.; Carmen, G.; Kerstin, K. *Angew Chem Int Ed* 2005, 44, 5188.
12. Hartmuth, C.; Kolb, M. G.; Finn, K.; Barry, S. *Angew Chem Int Ed* 2001, 40, 2004.
13. Metin, A.; Burcin, G.; Baris, K. *Polymer* 2008, 49, 2202.
14. Zeng, K.; Wang, L.; Zheng, S. X. *J Phys Chem B* 2009, 113, 11831.
15. Kuo, S. W.; Tsai, H. T. *Polymer* 2010, 51, 5695.
16. Benjamin, I. D.; Hernan, R. R.; Nicholas, J. T. *Macromolecules* 2010, 43, 6549.
17. Wolfgang, H. B.; Laura, P.; Robert, S. *Monatsh Chem* 2006, 137, 835.
18. Shen, D. M.; Liu, C.; Chen, Q. Y. *Eur J Org Chem* 2007, 1419.
19. Vegar, S.; Anne, F. *Tetrahedron* 2008, 64, 7626.
20. Batog, L. V.; Konstantinova, L. S.; Rozhkov, V. Y. *Russ Chem Bull* 2005, 54, 1915.
21. Beatriz, T.; Roberto, S. *Chem Eur J* 2010, 16, 3833.
22. Liu, Q.; Yitzhak, T. *Org Lett* 2003, 5, 2571.
23. Fan, H. B.; Yang, R. J. *Polym Mater Sci & Eng*, accepted.
24. Du, J. K. Doctoral Dissertation of Beijing Institute of Technology, 2006.
25. Hu, C. W. University Chemistry; Chemical Industry Press: Beijing, 2009.
26. Huang, J. C.; He, C. B.; Xiao, Y.; Mya, K. Y.; Dai, J.; Siow, Y. P. *Polymer* 2003, 44, 4494.
27. Zhang, J.; Xu, R. W.; Yu, D. S. *Eur Polym J* 2007, 43, 743.
28. Zhang, J. L.; Pang, S. P.; Li, Y. C. *Chin J Energetic Mater* 2006, 14, 355.
29. Qi, W. M. *Chemical Eng Equipment* 2010, 6, 156.
30. Wu, C. S.; Liu, Y. L.; Chiu, Y. C.; Chiu, Y. S. *Polym Degrad Stab* 2002, 78, 41.
31. Liu, Y. L.; Chou, C. I. *Polym Degrad Stab* 2005, 90, 515.